

## Tailoring Structure–Property Relationships in Dithienosilole–Benzothiadiazole Donor–Acceptor Copolymers

Pierre M. Beaujuge,<sup>†</sup> Wojciech Pisula,<sup>‡</sup> Hoi Nok Tsao,<sup>‡</sup> Stefan Ellinger,<sup>†</sup>  
Klaus Müllen,<sup>\*,‡</sup> and John R. Reynolds<sup>\*,†</sup>

The George and Josephine Butler Polymer Research Laboratory, Center for Macromolecular Science and Engineering, Department of Chemistry, University of Florida, Gainesville, Florida 32611, and Max Planck Institute for Polymer Research, Ackermannweg 10, D-55128 Mainz, Germany

Received January 22, 2009; E-mail: reynolds@chem.ufl.edu; muellen@mpip-mainz.mpg.de

First introduced in 1993 by Havinga et al. in macromolecular systems,<sup>1</sup> the donor–acceptor approach has proved remarkably effective in the synthetic design of narrow band gap  $\pi$ -conjugated polymers absorbing at longer wavelengths than their wider band gap all-donor counterparts (e.g., P3HT, MEH-PPV, and MDMO-PPV).<sup>2</sup> In solar cells for instance, the ability to harvest light over the range of wavelengths where the photon flux is maximum (i.e., 500–800 nm) is determining.<sup>3</sup> However, absorption of sunlight is far from being the only parameter of importance, and the charge transport taking place across the devices remains the primary factor governing their performance.<sup>3b</sup> While broadly absorbing polymers with excellent charge-carrier mobilities are highly desired for photovoltaic applications, their synthetic access has remained challenging so far.<sup>4</sup>

A recent report from Yang et al. describing a strictly alternating DA copolymer of dithieno[3,2-*b*:2',3'-*d*]silole (DTS) and 2,1,3-benzothiadiazole (BTD) with power conversion efficiencies as high as 5.1% (AM 1.5) in solar cells<sup>5</sup> is prompting us to report on the synthesis and structure–property relationships of a series of novel DTS–BTD copolymers (**P1**, **P2**, **P3**, and **P4**) attaining unusually broad spectral absorptions (see Figure 1) and hole mobilities as

making broadly absorbing polymer electrochromes, whereby long segments of electron-donating heterocycles space the electron-deficient units, producing two optical transitions which evolve toward balancing their intensities and coalesce with increasing number of donors.<sup>7</sup> As predicted, **P2**, **P3**, and **P4** absorb the visible light more effectively than the control polymer **P1** with **P4** exhibiting the most extended and homogeneous spectrum of all (see the red circled area in the range 400–550 nm).

Scheme 1 outlines our synthetic strategy for combining the fused donor DTS with the acceptor BTD into copolymers with electron-

### Scheme 1. Synthetic Route to Copolymers P1–P4

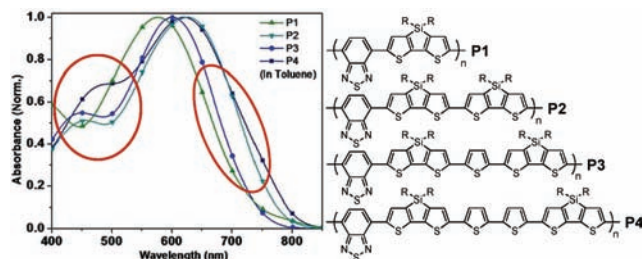
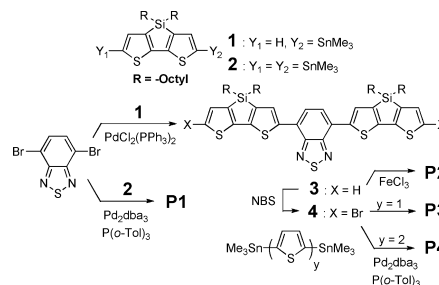


**Figure 1.** Normalized Solution optical absorption and structures of DTS–BTD copolymers **P1**, **P2**, **P3**, and **P4**.

high as  $0.02 \text{ cm}^2 \text{ V}^{-1} \text{ s}^{-1}$  in solution deposited bottom-contact FETs. Here we provide insight into how careful structural modifications can be used to tailor the spectrum and charge-carrier mobilities of  $\pi$ -conjugated polymers simultaneously.

Inspired by work from Marks et al. on silole-based copolymers with high-performance in field-effect transistors (FETs),<sup>6</sup> our synthetic design combines the use of electron-rich DTS and unsubstituted thiophene spacers with the donor–acceptor approach (via BTD) to produce polymers absorbing across the entire visible spectrum. The wide absorption bandwidths seen in Figure 1 were achieved by applying a strategy recently reported by our group for

rich segments of various lengths, hence progressively dispersing BTD along the main chains. The synthetic details can be found in the Supporting Information. In brief, polymers **P1**, **P3**, and **P4** were synthesized via Stille-type polycondensations in hot mixtures of toluene and DMF (80–95 °C) using  $\text{Pd}_2\text{dba}_3$ ,  $\text{P}(o\text{-Tol})_3$  as the catalyst. **P2** was oxidatively polymerized at room temperature using  $\text{FeCl}_3$  and subsequently reduced with hydrazine. The polymer structures were supported by  $^1\text{H}$ ,  $^{13}\text{C}$  NMR and elemental analysis. Table 1 summarizes the molecular weights obtained by GPC and

**Table 1.** Number Average Molecular Weight ( $M_n$ , kDa), Polydispersity (PDI), Optical Band Gap ( $E_g$ , eV),  $\pi$ -Stacking ( $\pi$ , nm) and Chain-to-Chain Distances ( $d$ , nm), FET Charge Carrier Mobilities at Saturation ( $\mu_{\text{sat}}$ ,  $\text{cm}^2 \text{ V}^{-1} \text{ s}^{-1}$ ), and Current On/Off Ratios ( $I_{\text{on}}/I_{\text{off}}$ ) for Copolymers **P1** (on PTES-Treated  $\text{SiO}_2$ ) and **P2–P4** (on HMDS-Treated  $\text{SiO}_2$ )

polymer	$M_n$ (PDI)	$E_g$	$\pi$ ( $d$ )	$\mu_{\text{sat}}$	$I_{\text{on}}/I_{\text{off}}$
<b>P1</b>	10.8 (3.2)	1.53	– (1.95)	$2 \times 10^{-6}$	$1 \times 10^2$
<b>P2</b>	17.7 (3.3)	1.53	0.36 (1.95)	$3 \times 10^{-4}$	$6 \times 10^3$
<b>P3</b>	16.0 (3.8)	1.56	– (1.94)	$3 \times 10^{-3}$	$2 \times 10^4$
<b>P4</b>	19.8 (3.2)	1.51	0.36 (1.84)	$2 \times 10^{-2}$	$1 \times 10^3$

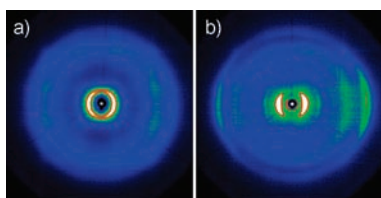
the band gaps as measured from the onset of their low-energy optical absorption (1.51–1.56 eV). Note that the  $M_n$  values of **P3** and **P4** are greater than that of **P1**, yet all polymers show a polymerization degree superior or equal to 15 (**P3**) and a minimum average of 57 rings (**P1**).

<sup>†</sup> University of Florida.

<sup>‡</sup> Max Planck Institute for Polymer Research.

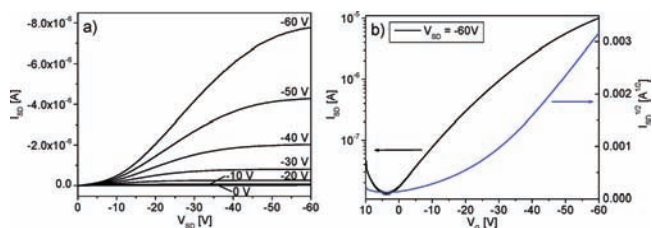
The organization of the copolymers was investigated by fiber X-ray scattering, whereby the samples were prepared by mechanical extrusion.<sup>8</sup> The X-ray data are summarized in Table 1. **P1** and **P2** organize in lamellae structures with an identical chain-to-chain distance of 1.95 nm as derived from the small-angle equatorial reflections (see Figure S1). However, the isotropic small-angle reflection and the lack of corresponding scattering intensity in the pattern of **P1** translate into an absence of  $\pi$ -stacking. In contrast, the wide-angle reflections in the equatorial plane of the pattern of **P2** correspond to  $\pi$ -stacking distances of 0.36 nm, hence pointing toward improved order. The field-effect transistor (FET) performance data are summarized in Table 1. Bottom contact FETs were obtained by drop-casting both copolymers from a 2 mg mL<sup>-1</sup> chlorobenzene solution on HMDS-treated SiO<sub>2</sub> covering heavily doped Si as the gate electrode. In correlation with their differences in organization, compound **P1** did not show any transistor behavior, while **P2** revealed a clear field-effect with a moderate hole mobility of  $3 \times 10^{-4}$  cm<sup>2</sup> V<sup>-1</sup> s<sup>-1</sup> at saturation and an on/off current ratio of  $6 \times 10^3$ . However, by substituting HMDS with phenyltriethoxysilane (PTES), **P1** then revealed a very limited hole mobility of  $2 \times 10^{-6}$  cm<sup>2</sup> V<sup>-1</sup> s<sup>-1</sup> at saturation and an on/off current ratio of  $1 \times 10^2$ .

Figure 2a and 2b show characteristic 2D X-ray patterns for **P3** and **P4**, respectively. Similarly to **P1**, copolymer **P3** revealed



**Figure 2.** 2D wide-angle X-ray scattering (2D-WAXS) of (a) **P3** and (b) **P4**.

reflections corresponding to the lamellar spacing only (1.94 nm). The distinct scattering intensities in the pattern of **P4** demonstrate a higher degree of crystallinity and alignment of the lamellae structures along the fiber direction. **P4** shows a chain-to-chain spacing of 1.84 nm and  $\pi$ -stacking distances of 0.36 nm which represent, to the best of our knowledge, some of the closest intermolecular interactions reported to date for a solution-processable polymer.<sup>9</sup> In spite of the lack of organization in **P3**, a better FET performance than that of **P1** and **P2** with a hole mobility of  $3 \times 10^{-3}$  cm<sup>2</sup> V<sup>-1</sup> s<sup>-1</sup> at saturation and an on/off current ratio of  $2 \times 10^4$  was found, hence supporting the favorable effect of inserting bare heterocyclic units in the copolymer backbones to enhance the carrier mobilities.<sup>6</sup> With the increase of order and molecular packing of **P4**, an enhanced hole mobility of 0.02 cm<sup>2</sup> V<sup>-1</sup> s<sup>-1</sup> at saturation and an on/off current ratio of  $1 \times 10^3$  were obtained as illustrated in Figure 3. We attribute the close intermolecular distances in **P4**



**Figure 3.** Field-effect transistor characteristics of **P4**: (a) output curves taken at different gate voltages and (b) transfer curves.

and FET performance enhancement to the presence of unsubstituted bithiophene spacers creating effective hopping sites for the charge carriers, reducing the concentration of solubilizing groups and increasing the coplanarity of the backbone.

Interestingly, in spite of its close  $\pi$ -stacking distance, the mobility of **P2** was 2 orders of magnitude lower than that of **P4**, which can be explained by the lower degree of crystallinity evidenced by the relatively broad reflections and the lack of higher order scattering intensities in the corresponding 2D pattern. Importantly, the same trend was observed by X-ray diffraction in thin films (see Figure S2), where **P4** showed the highest extent of crystallinity, while the X-ray diffractogram of **P2** exhibited only a weak reflection indicative of a poor degree of macroscopic order. Identical  $d$ -spacings were determined for the thin films and from the bulk, suggesting no variation in the molecular packing upon thin film processing.

In conclusion, four new **DTS-BTD** copolymers differing by the concentration of electron-donating and -withdrawing substituents along the backbone have been synthesized and characterized by 2D-WAXS and in bottom-contact FETs. While all copolymers were able to self-assemble into lamellar superstructures, only **P2** and **P4** showed a propensity to  $\pi$ -stack. The highest hole mobility of 0.02 cm<sup>2</sup> V<sup>-1</sup> s<sup>-1</sup> was observed for **P4** in excellent agreement with the close  $\pi$ -stacking and lamellar distances found by structural analysis (0.36 and 1.84 nm, respectively). In parallel, **P4** absorbs homogeneously across the entire visible spectrum as solar cell applications require. The FET performance is expected to improve with controlled polymer molecular weight and macroscopic order.<sup>8c</sup>

**Acknowledgment.** The authors thank the AFOSR (FA9550-06-1-0192) for financial support. We appreciate the contribution of Unsal Koldemir in preparing starting material.

**Supporting Information Available:** **P1-P4** syntheses, X-ray patterns of **P1** and **P2**, and FET device fabrication details. This material is available free of charge via the Internet at <http://pubs.acs.org>.

## References

- Havinga, E. E.; Hoeve, W.; Wynberg, H. *Synth. Met.* **1993**, *55*, 299–306.
- (a) Wienk, M. M.; Turbiez, M.; Janssen, R. A. J. *Adv. Mater.* **2008**, *20*, 2556–2560. (b) Mühlbacher, D.; Scharber, M.; Morana, M.; Zhu, Z.; Waller, D.; Gaudiana, R.; Brabec, C. *Adv. Mater.* **2006**, *18*, 2884–2889. (c) Kim, J. Y.; Lee, K.; Coates, N. E.; Moses, D.; Nguyen, T.-Q.; Dante, M.; Heeger, A. J. *Science* **2007**, *317*, 222–225. (d) Ergang, W.; Li, W.; Linfeng, L.; Chan, L.; Wenliu, Z.; Junbiao, P.; Yong, C. *Appl. Phys. Lett.* **2008**, *92*, 033307. (e) Blouin, N.; Michaud, A.; Gendron, D.; Wakim, S.; Blair, E.; Neagu-Plesu, R.; Belletete, M.; Durocher, G.; Tao, Y.; Leclerc, M. *J. Am. Chem. Soc.* **2008**, *130*, 732–742. (f) Bundgaard, E.; Krebs, F. C. *Macromolecules* **2006**, *39*, 2823–2831.
- (a) Thompson, B. C.; Fréchet, J. M. J. *Angew. Chem., Int. Ed.* **2008**, *47*, 58–77. (b) Gunes, S.; Neugebauer, H.; Sariciftci, N. S. *Chem. Rev.* **2007**, *107*, 1324–1338.
- Li, Y.; Zou, Y. *Adv. Mater.* **2008**, *20*, 2952–2958.
- Hou, J.; Chen, H.-Y.; Zhang, S.; Li, G.; Yang, Y. *J. Am. Chem. Soc.* **2008**, *130*, 16144–16145.
- (a) Usta, H.; Lu, G.; Facchetti, A.; Marks, T. J. *J. Am. Chem. Soc.* **2006**, *128*, 9034–9035. (b) Usta, H.; Facchetti, A.; Marks, T. J. *J. Am. Chem. Soc.* **2008**, *130*, 8580–8581.
- Beaujuge, P. M.; Ellinger, S.; Reynolds, J. R. *Nat. Mater.* **2008**, *7*, 795–799.
- (a) Pisula, W.; Tomovic, Z.; Simpson, C.; Kastler, M.; Pakula, T.; Müllen, K. *Chem. Mater.* **2005**, *17*, 4296–4303. (b) Zhang, M.; Tsao, H. N.; Pisula, W.; Yang, C.; Mishra, A. K.; Müllen, K. *J. Am. Chem. Soc.* **2007**, *129*, 3472–3473. (c) Tsao, H. N.; Cho, D.; Andreasen, J. W.; Rouhanipour, A.; Breiby, D. W.; Pisula, W.; Müllen, K. *Adv. Mater.* **2009**, *21*, 209–212.
- (a) Osaka, I.; Sauvé, G.; Zhang, R.; Kowalewski, T.; McCullough, R. D. *Adv. Mater.* **2007**, *19*, 4160–4165. (b) McCulloch, I.; Heeney, M.; Bailey, C.; Genevicius, K.; MacDonald, I.; Shkunov, M.; Sparrow, D.; Tierney, S.; Wagner, R.; Zhang, W.; Chabynyc, M. L.; Kline, R. J.; McGehee, M. D.; Toney, M. F. *Nat. Mater.* **2006**, *5*, 328–333.

JA900519K